Turbulent saturation of two-dimensional curvature-driven ITG modes

P. G. Ivanov, A. A. Schekochihin,
W. Dorland, A. R. Field, F. I. Parra

July 29, 2019

Overview

- Understanding heat transport in tokamak plasmas is crucial for the design of future experiments and reactors
- Numerical evidence points towards turbulence as the main cause for heat transport in tokamak plasmas
- Therefore, we seek to describe the saturated turbulent state and the mechanisms of its saturation
- We focus on turbulence driven by the ITG instability

Turbulent saturation

- Strongly driven turbulence (i.e. far from marginal stability) is known to saturate via a "critically balanced" turbulent cascade (Barnes *et al.* 2011)
- Close to marginality, however, numerical simulations suggest that saturation is dominated by strong poloidal shear flows or "zonal flows" (ZF)
- ZFs help saturation by shearing drift-wave (DW) eddies

Overview

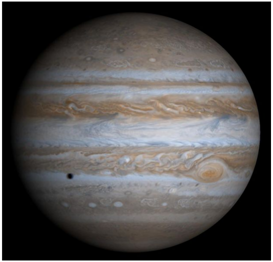

Figure: Zonal flows on Jupiter (Photo by NASA).

- Similar shear flows are seen in other contexts, most notably the atmosphere of Jupiter

Goals

- Find a simplified model for ZF-DW interactions, which allows us to make analytical as well as numerical progress
- Determine the mechanism of zonal regulation in the near-marginal ("Dimits") regime and the reason for its collapse

Requirements

- A linear ITG instability with no external forcing or artificial dissipation
- Correct electron physics — modified adiabatic response:

$$\delta n_e = \frac{e(\phi - \overline{\phi})}{T_e} = \frac{e\phi'}{T_e}, \tag{1}$$

  where $\overline{\phi}$ is the flux-surface (zonal) average of ϕ and $\phi' \equiv \phi - \overline{\phi}$ is the nonzonal (drift-wave) part of the field
- 2D is not essential (some might view it as too restrictive), but it allows analytic progress
- An asymptotic limit of the ion gyrokinetic equation in some physical regime, rather than ad hoc

Magnetic and thermal equilibrium

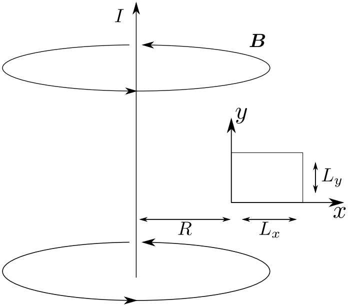

Figure: Visualisation of the magnetic geometry and domain location.

Define magnetic and temperature gradients:

$$L_B^{-1} = -\partial_x \ln B, \quad L_T^{-1} = -\partial_x \ln T_i. \tag{2}$$

Zonal averages are

$$\overline{f}(x) = \frac{1}{L_y} \int dy \; f(x, y). \tag{3}$$

Approximations

- High-collisionality, long-wavelength

$$\nu_i \gg \partial_t \sim k_\perp^2 \rho_i^2 \nu_i, \; k_\perp^2 \rho_i^2 \ll 1. \tag{4}$$

- Cold ions $T_i/T_e \to 0$, but finite sound radius

$$\rho_s \equiv \frac{\rho_i}{\sqrt{2\tau}}, \; \tau \equiv \frac{T_i}{ZT_e}. \tag{5}$$

Applying these approximations to the ion gyrokinetic (GK) equation (Frieman & Chen 1982), we obtain a system of closed equations for the electric potential ϕ and ion temperature perturbations δT_i.

2D 2-fluid ITG Model

$$\partial_t \left(\varphi' - \nabla^2\varphi\right) + \left\{\varphi, \varphi' - \nabla^2\varphi\right\} + \nabla \cdot \{\nabla\varphi, T\}$$
$$- \partial_y \left(\varphi + T\right) + \kappa_T \partial_y \nabla^2 \varphi = -\chi \nabla^4 (a\varphi - bT), \tag{6}$$

$$\partial_t T + \{\varphi, T\} + \kappa_T \partial_y \varphi = \chi \nabla^2 T. \tag{7}$$

$\varphi = \dfrac{\tau L_B}{2\rho_s} \dfrac{Z_i e \phi}{T_i}$ is the normalised electric potential,

$T = \dfrac{\tau L_B}{2\rho_s} \dfrac{\delta T}{T_i}$ is the normalised ion temperature perturbation,

$\kappa_T \equiv \dfrac{\tau L_B}{2 L_T}$ is the normalised equilibrium ion temperature gradient,

$\chi \equiv \dfrac{L_B}{\Omega_i \rho_s^3} \dfrac{4}{9} \sqrt{\dfrac{2}{\pi}} \nu_i \rho_i^2$ is the heat diffusivity, and $a = \dfrac{9}{40}$, $b = \dfrac{67}{160}$.

2D 2-fluid ITG Model

$$\partial_t \left(\varphi' - \nabla^2\varphi\right) + \left\{\varphi, \varphi' - \nabla^2\varphi\right\} + \nabla\cdot\{\nabla\varphi, T\} \\ - \partial_y\left(\varphi + T\right) + \kappa_T\partial_y\nabla^2\varphi = -\chi\nabla^4(a\varphi - bT),$$

$$\partial_t T + \{\varphi, T\} + \kappa_T\partial_y\varphi = \chi\nabla^2 T.$$

$t \equiv \dfrac{2\rho_s\Omega_i}{L_B} t_{\mathrm{phys}}$ is normalised to the magnetic drift frequency,

$x \equiv \dfrac{x_{\mathrm{phys}}}{\rho_s}$, $y \equiv \dfrac{y_{\mathrm{phys}}}{\rho_s}$ are normalised the radial and poloidal coords.

The Poisson bracket is $\{f, g\} = \partial_x f\partial_y g - \partial_y f\partial_x g = \hat{\boldsymbol{z}}\cdot(\nabla f\times\nabla g)$

The only parameters are κ_T, χ and the size of the domain.

ITG Instability

Dispersion relation for a mode with $\varphi, T \propto e^{-i\omega t + i\boldsymbol{k}\cdot\boldsymbol{r}}$:

$$\begin{aligned} -\omega^2(1+k^2) - i\omega\left[-ik_y(1+\kappa_T k^2) + i\chi k^2\left(1+(1+a)k^2\right)\right] \\ + a\chi^2 k^6 - \kappa_T k_y^2 - ik_y\chi k^2\left(1+\kappa_T(1-b)k^2\right) = 0. \end{aligned} \tag{8}$$

Quite involved, in the limit $k^2 \ll \kappa_T^{-1/2} \ll 1$ we find

$$\mathrm{Im}\ \omega \approx k_y\sqrt{\kappa_T}, \tag{9}$$

which transformed to dimensional units gives the familiar

$$\mathrm{Im}\ \omega_{\mathrm{phys}} = \Omega_i \frac{\rho_i^2 k_{y,\ \mathrm{phys}}}{\sqrt{2\tau L_B L_T}}. \tag{10}$$

ITG Instability

- Modes are always damped for large k^2
- Two independent cut-off mechanisms — finite Larmor radius effects and collisions
- Assuming ideal cases, we obtain two limits on k^2:

$$k^2_{\text{max, FLR}} = \frac{1 + 2\sqrt{\kappa_T}}{\kappa_T}, \tag{11}$$

$$k^2_{\text{max, }\chi} = \left(\frac{\kappa_T k_y^2}{a\chi}\right)^{1/3}. \tag{12}$$

ITG Instability

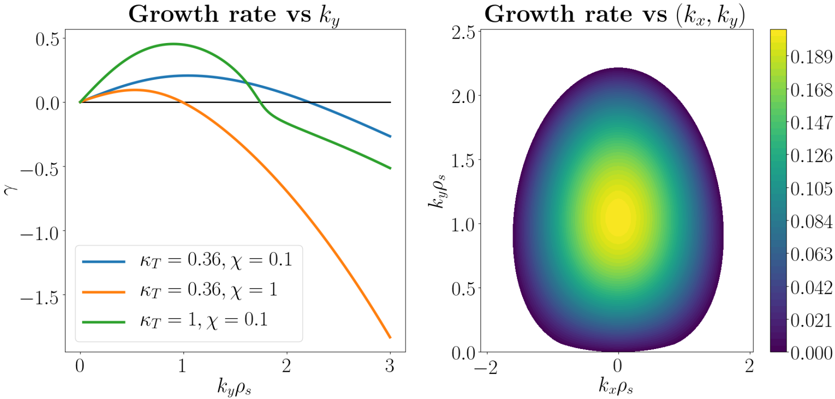

Figure: Linear growth rates of pure DW ($k_x = 0$) Fourier modes.

Conservation Laws

The equations above have the following conservation laws:

$$\partial_t \int dxdy\ \frac{1}{2}T^2 = \kappa_T \int dxdy\ T\partial_y\varphi - \chi \int dxdy\ \left(\nabla T\right)^2, \quad (13)$$

$$\partial_t \int dxdy\ \frac{1}{2}\left[{\varphi'}^2 + (\nabla\varphi)^2\right]$$

$$= \int dxdy\ T\partial_y\varphi + \chi \int dxdy\ (\nabla^2\varphi)\left(a\nabla^2\varphi - b\nabla^2 T\right), \quad (14)$$

$$\partial_t \int dxdy\ \left[\frac{1}{2}{\varphi'}^2 + T\varphi' + \frac{1}{2}\left(\nabla T + \nabla\varphi\right)^2\right]$$

$$= -\chi \int dxdy\ \Big[\left(\nabla\varphi'\right)\cdot\left(\nabla T\right) + a\left(\nabla^2\varphi\right)^2$$

$$+\ (1+a-b)\left(\nabla^2\varphi\right)\left(\nabla^2 T\right) + (1-b)\left(\nabla^2 T\right)^2\Big]. \quad (15)$$

Relationship to the Charney-Hasegawa-Mima equation

- Setting $\kappa_T = 0,\ T = 0$ collapses our equations to the Charney-Hasegawa-Mima (CHM) equation (Hasegawa & Mima 1978)

$$\partial_t \left(\varphi' - \nabla^2\varphi\right) + \left\{\varphi, \varphi' - \nabla^2\varphi\right\} - \partial_y\varphi = -a\chi\nabla^4\varphi. \tag{16}$$

- So our model is effectively CHM with a linear instability, cf. Hasegawa & Wakatani (1983) and Terry & Horton (1983)

Numerical solution

We proceed to integrate the equations above using a pseudo-spectral algorithm, very similar to the GS2 one.

Let's watch a film...

Quasi-steady Saturation

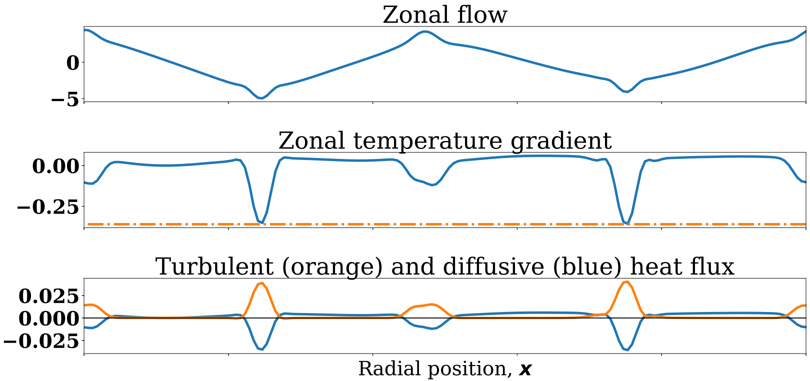

Figure: Zonal profiles for $\chi = 0.1, \kappa_T = 0.36$.

Quasi-steady Saturation

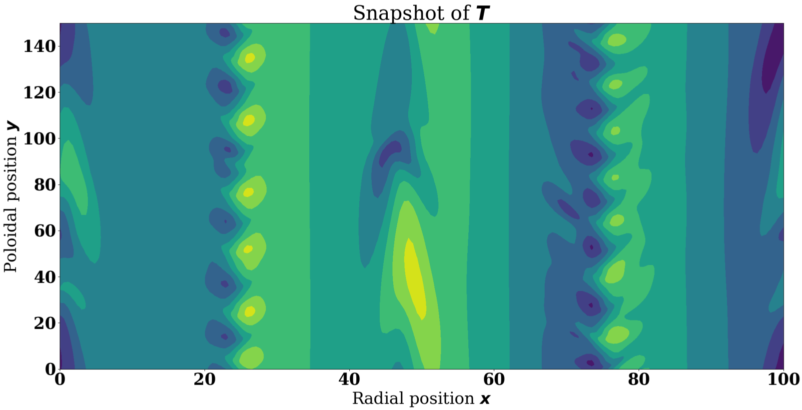

Figure: Temperature perturbations for $\chi = 0.1, \kappa_T = 0.36$.

Quasi-steady Saturation

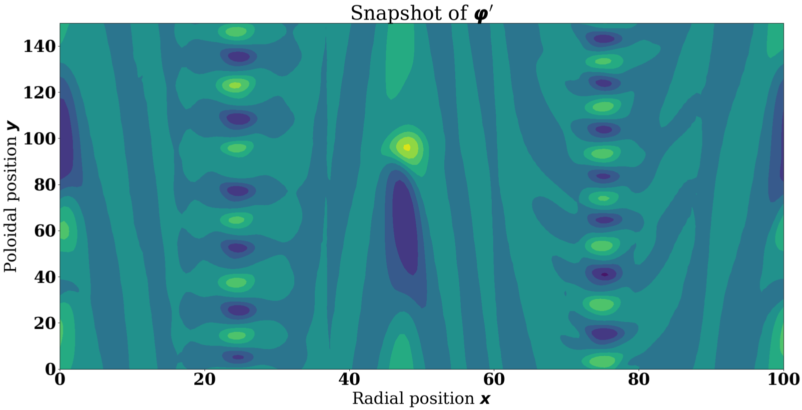

Figure: Nonzonal potential, φ', for $\chi = 0.1, \kappa_T = 0.36$.

Quasi-steady Saturation

- Zonal shear suppresses DWs throughout most of the domain
- Localised patches of DW turbulence exist in the regions, where shear vanishes
- The temperature gradient is flattened in the turbulent regions (cf. Rayleigh–Bénard convection)
- Reminiscent of the "ExB" staircase

Quasi-steady Saturation

However, this state is not steady...

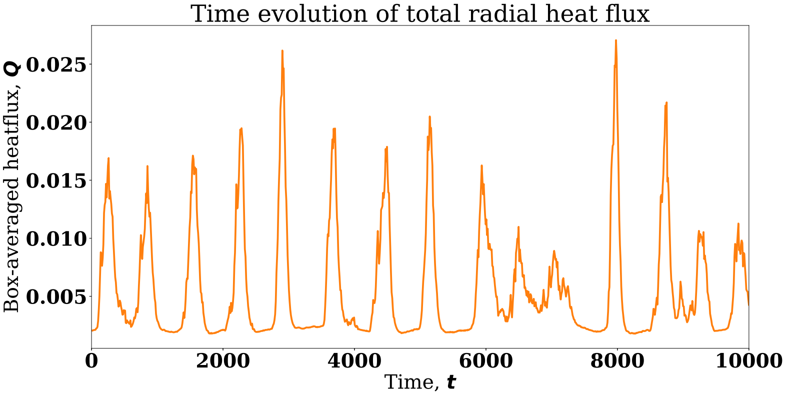

Figure: Heat flux time evolution for $\kappa_T = 0.36, \chi = 0.1$.

Quasi-steady Saturation

The ZF and zonal temperature evolution equations are

$$\partial_t \overline{\varphi} = \underbrace{\overline{\partial_x \varphi \partial_y (\varphi + T)}}_{\equiv \Pi(x), \text{ turb. pol. mom. flux}} + \underbrace{\partial_x^2 (a\overline{\varphi} - b\overline{T})}_{\text{diffusive pol. mom. flux}} ,$$

$$\partial_t \overline{T} = \partial_x \left(\underbrace{\overline{T \partial_y \varphi}}_{\equiv Q_r(x), \text{ turb. rad. heat flux}} + \underbrace{\chi \partial_x \overline{T}}_{\text{diffusive rad. heat flux}} \right).$$

Total radial heat flux through the domain is

$$Q = \frac{1}{L_x} \int dx \; Q_r(x) = \frac{1}{L_x L_y} \int dx dy \; T \partial_y \varphi.$$

Suppressing Turbulence

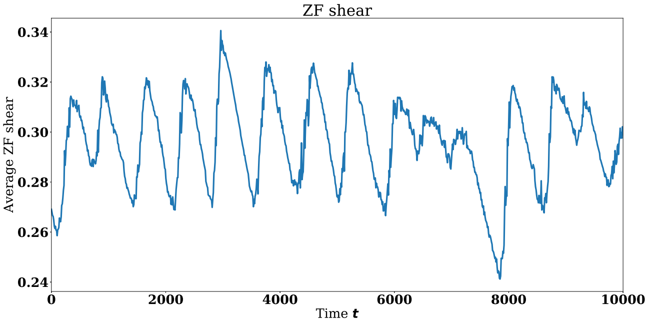

Figure: Variation of zonal shear, $\partial_x^2 \overline{\varphi}$, in constant-shear regions.

- A particular value of zonal shear is needed to suppress turbulence
- ZFs, and with them their shear, decay slowly due to viscosity
- A burst of turbulence re-establishes the zonal profile

Decay of ZF

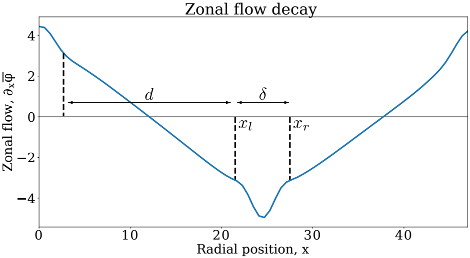

Figure: Estimation of shear decay rate.

$$\partial_t \int_{x_l}^{x_r} dx \partial_x \overline{\varphi} \approx a\chi \partial_x^2 \overline{\varphi}\Big|_{x_l}^{x_r} = 2a\chi s, \text{ where } s = \partial_x^2 \varphi \text{ is ZF shear.}$$

$$\partial_t \int_{x_l}^{x_r} dx \partial_x \overline{\varphi} = \frac{1}{2}\delta d \partial_t s$$

$$\implies s = s_0 \exp\left(-\frac{4a\chi}{d\delta} t\right).$$

Decay of ZF

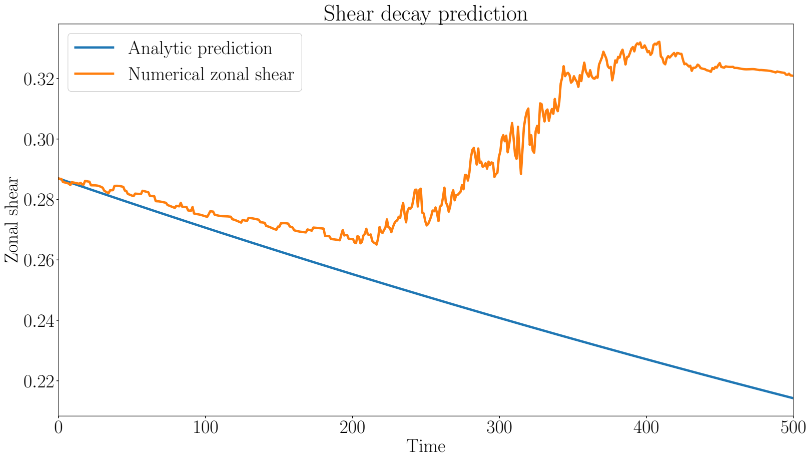

Figure: Numerical validation of shear decay mechanism.

Localised Structures

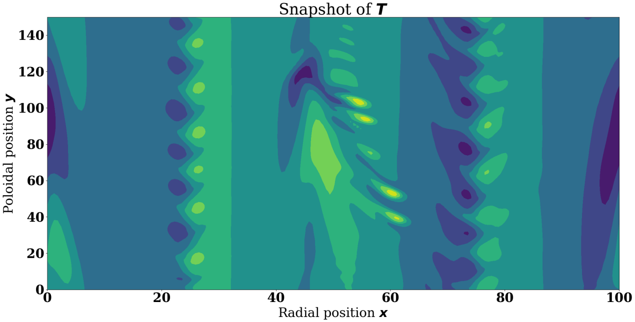

Figure: Snapshot of T with structures visible.

- Coherent structures (cf. van Wyk *et al.* 2017) are seen drifting through the sheared regions
- ZFs fairly undisturbed
- These structures increase heat flux dramatically

Localised Structures

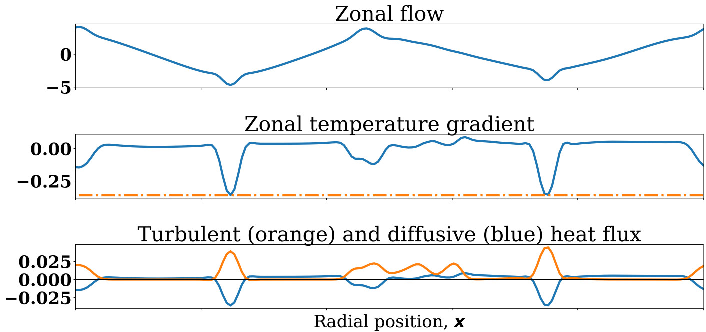

Figure: Zonal fields with structures.

- Coherent structures (cf. van Wyk *et al.* 2017) are seen drifting through the sheared regions
- ZFs fairly undisturbed
- These structures increase heat flux dramatically

Stability of Zonal Profiles

Let us investigate the stability of the zonal shear profile. The poloidal momentum equation gives

$$\partial_t \overline{\varphi} = \overline{\partial_x \varphi \partial_y \left(\varphi + T\right)} + \chi \partial_x^2 (a\overline{\varphi} - b\overline{T}). \qquad (17)$$

Now suppose we let DW turbulence saturate over this zonal shear background. Does its turbulent momentum flux restore or relax the zonal profile?
We investigate the behaviour of $\overline{\partial_x \varphi \partial_y \varphi}$ and $\overline{\partial_x \varphi \partial_y T}$ separately.

Stability of Zonal Profiles

Drift-wave turbulence over a zonal background satisfies the following equations:

$$
\begin{aligned}
&(\partial_t + \underline{\partial_x \overline{\varphi} \partial_y}) \left(1 - \nabla^2\right) \varphi' - (1 \underline{- \partial_x^3 \overline{\varphi}}) \partial_y \left(\varphi' + T'\right) + \kappa_T \partial_y \nabla^2 \varphi' \\
&\quad \underline{+ \partial_x^2 \overline{\varphi} \partial_x \partial_y T'} + \left\{\varphi', -\nabla^2 \varphi'\right\} + \nabla \cdot \left\{\nabla \varphi', T'\right\} \\
&\quad = -\chi \nabla^4 (a\varphi' - bT'),
\end{aligned} \tag{18}
$$

$$
(\partial_t + \underline{\partial_x \overline{\varphi} \partial_y}) T' + \kappa_T \partial_y \varphi' + \left\{\varphi', T'\right\} = \chi \nabla^2 T', \tag{19}
$$

where the highlighted terms are the ZF interaction terms.

Stability of Zonal Profiles

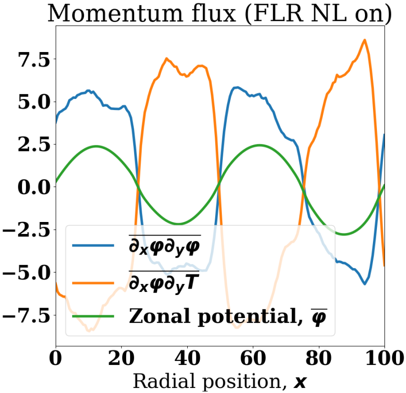

Figure: Momentum flux for DW turbulence over a fixed zonal background.

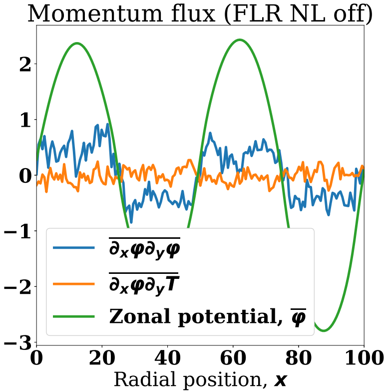

Figure: Momentum flux with $\overline{\partial_x\varphi\partial_y T}$ turned off.

Stability of Zonal Profiles

Consider a zonal profile of constant zonal shear $\partial_x^2 \overline{\varphi} = s = \text{const}$. We can eliminate the shear term $\partial_t + sx\partial_y$ by changing coordinates to the "shearing frame"

$$t' = t, x' = x,\ y' = y - stx$$
$$\implies \partial_t = \partial_{t'} - sx\partial_{y'},\ \partial_y = \partial_{y'},\ \partial_x = \partial_{x'} - st\partial_{y'}.$$

For a Fourier mode, which keeps its structure in the shearing frame, we obtain

$$k_y = k_{y'},\ k_x = k_{x'} - stk_{y'}. \tag{20}$$

Perturbations "drift" in Fourier space due to the zonal shear.

Stability of Zonal Profiles

We can write

$$\int dx\ \overline{\partial_x \varphi \partial_y \varphi} = \sum_{\boldsymbol{k}} k_x k_y |\varphi_k|^2 \tag{21}$$

- For $s > 0$ get positive k_y associated with negative k_x and vice-versa.
- For $s < 0$ get the opposite
- Thus s and $\int dx\ \overline{\partial_x \varphi \partial_y \varphi}$ have opposite signs
- So $\overline{\varphi}$ and $\int dx\ \overline{\partial_x \varphi \partial_y \varphi}$ have the same sign

Stability of Zonal Profiles

Using the conservations laws for drift-wave fields in constant zonal shear profile, we can write

$$s \int dx \, \overline{\partial_x \varphi \partial_y T} = \int dxdy \left[a \left(\nabla^2 \varphi' \right)^2 - b \left(\nabla^2 \varphi' \right) \left(\nabla^2 T \right) - \frac{1}{\kappa_T} \left(\nabla T \right)^2 \right]$$

$$+ \partial_t \int dxdy \left[\varphi'^2 + \left(\nabla \varphi' \right) - \frac{1}{\kappa_T} T^2 \right]$$

- In a saturated state $\partial_t \approx 0$
- Numerically we find that the b term is negligible
- With shear imposed we expect $\left(\nabla^2 \varphi' \right)^2$ to dominate

Hence

$$s \int dx \, \overline{\partial_x \varphi \partial_y T} > 0. \tag{22}$$

Stability of Zonal Profiles

We find that increasing the temperature gradient κ_T eventually leads to a break up of the zonal state.

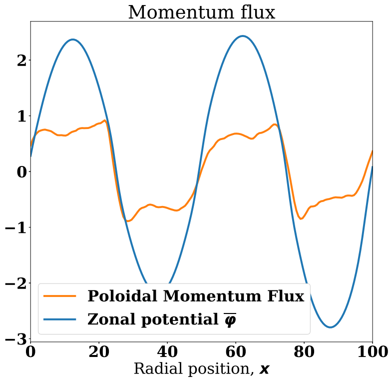

Figure: Stable $\chi = 0.5, \kappa_T = 1$.

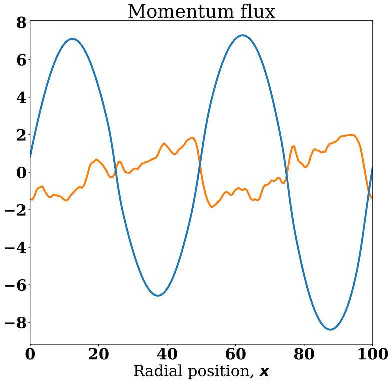

Figure: Unstable $\chi = 0.5, \kappa_T = 4$

- Beyond the staircase state, the system fails to reach saturation
- Hypothesis: the transition from saturation to blowup in this system is equivalent to the transition from the zonally-dominated Dimits regime to fully developed turbulence, seen in GK simulations (Dimits 2000)
- Failure to reach saturation in such a state is typical for 2D systems, since the additional conservation laws in 2D canoften overconstrain the system and lead to anomalies (cf.inverse energy cascade in hydrodynamics)
- Saturation in GK simulations beyond Dimits is "critically balanced" (Barnes *et al*, 2011), hence fundamentally 3D

Parameter space

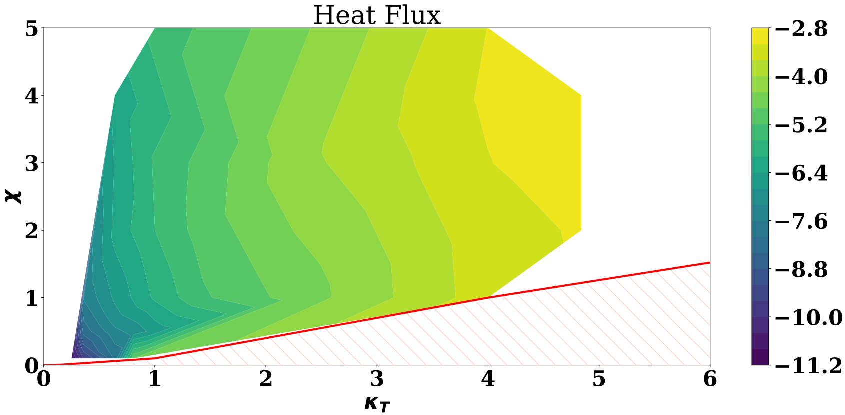

Figure: Visualisation of different regions of parameter space.

Parameter dependence of heat flux

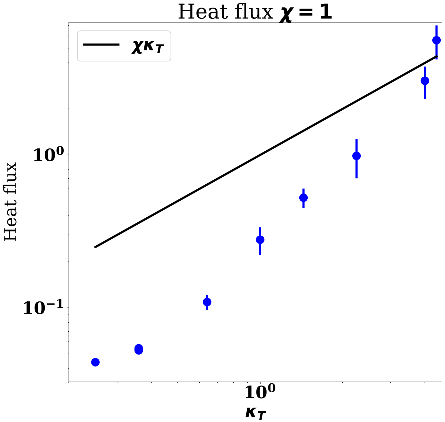

Figure: Heat flux vs κ_T.

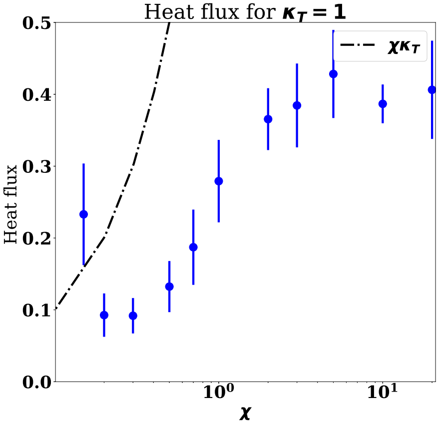

Figure: Heat flux vs χ.

Conclusions

- Dimits saturation in 2D turbulence relies on the formation of an ExB staircase
- Time-averaged heat flux is dominated by "predator-prey"-like oscillations of bursts of turbulence
- Coherent structures, which survive background shear, are found

Ideas for the future:

- More analytics in 2D — end of Dimits, coherent structures
- Investigate whether these ideas survive the chaos of 3D gyrokinetics

Here be supplementary slides

Secondary Instability

How are ZFs generated?

- Zonal ($k_y = 0$) modes are linearly stable
- The fastest growing linear ITG mode is a pure DW, i.e. $k_x = 0$
- The secondary instability is that of DWs to infinitesimal ZF perturbations

Secondary Instability

Taking a 4-mode truncation

$$\varphi = 2\mathrm{Re}\ \left[\varphi_q e^{iqy} + \left(\varphi_1 e^{iqy} + \varphi_{-1} e^{-iqy} + \varphi_0\right) e^{ipx} e^{\gamma_2 t}\right],$$

we find

$$\left(\gamma_2^2 + p^2 q^2 U\right)\left(\gamma_2^2 + p^2 q^2 V\right) = p^4 q^4 W,\ \text{where}$$

$$U = 2|\varphi_q|^2 + \frac{2q^2 \mathrm{Re}\ (\varphi_q T_q^*)}{1 + p^2 + q^2},$$

$$V = \frac{2\left[(p^2 - q^2 - 1)|\varphi_q|^2 + p^2 |T_q|^2 + (2p^2 - q^2 - 1)\mathrm{Re}\ (\varphi_q T_q^*)\right]}{1 + p^2 + q^2},$$

$$W = \frac{4p^2 q^2}{(1 + p^2 + q^2)^2}\left[|T_q|^2 + 2\mathrm{Re}\ (\varphi_q T_q^*)\right]\left[|\varphi_q|^2 + \mathrm{Re}\ (\varphi_q T_q^*)\right].$$

For $T = 0$ this collapses to the usual Hasegawa-Mima secondary

$$\gamma_2^{HM} = pq|\varphi_q|\sqrt{\frac{2(1 + q^2 - p^2)}{1 + p^2 + q^2}}.$$

Secondary Instability

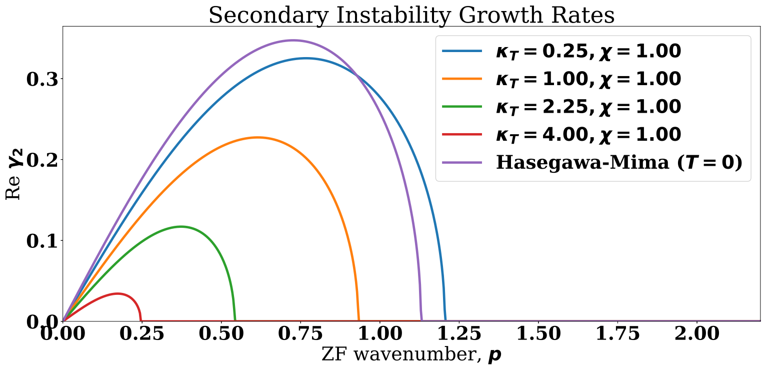

Figure: Secondary instability growth rates over the most unstable DW mode.

- Increasing κ_T decreases the secondary growth rate and span in Fourier space
- This diminished instability strongly resembles the ETG secondary of the CHM equation (with adiabatic ion response)

$$\gamma_2^{HM,ETG} = pq|\varphi_q|\sqrt{\frac{2p^2}{1+p^2}\frac{q^2-p^2}{1+p^2+q^2}}.$$

- Fluid ETG *often* fails to saturate. This has been associated with its secondary instability (Dorland *et al.* 2000)
- In our system ETG *always* fails to saturate, but the role of the secondary is unclear

Zonal Stability (linear)

Let us linearise the system for an infinitesimal DW perturbation over strong zonal fields. We refrain from using a 4-mode model.

$$(\partial_t + \partial_x\overline{\varphi}\partial_y)\left(1-\nabla^2\right)\varphi' - (1-\partial_x^3\overline{\varphi})\partial_y\left(\varphi' + T'\right) + (\kappa_T - \partial_x\overline{T})\partial_y\nabla^2\varphi' + \partial_x^2\overline{\varphi}\partial_x\partial_y T' - \partial_x^2\overline{T}\partial_x\partial_y\varphi' \quad = -\chi\nabla^4(a\varphi' - bT'), \tag{23}$$

$$(\partial_t + \partial_x\overline{\varphi}\partial_y)T' + (\kappa_T - \partial_x\overline{T})\partial_y\varphi' + \left\{\varphi', T'\right\} = \chi\nabla^2 T', \tag{24}$$

where the highlighted terms are the ZF interaction terms. We can heuristically understand the results by Rogers & Dorland (2000)

$$\gamma_3 \propto k_y\sqrt{\partial_x^3\overline{\varphi}(x_0)\partial_x\overline{T}(x_0)} \tag{25}$$

in a region where $\partial_x^2\overline{\varphi} = \partial_x^2\overline{T} = 0$.

Highly dissipative regime

Increasing collisionality leads to oscillating zonal fields

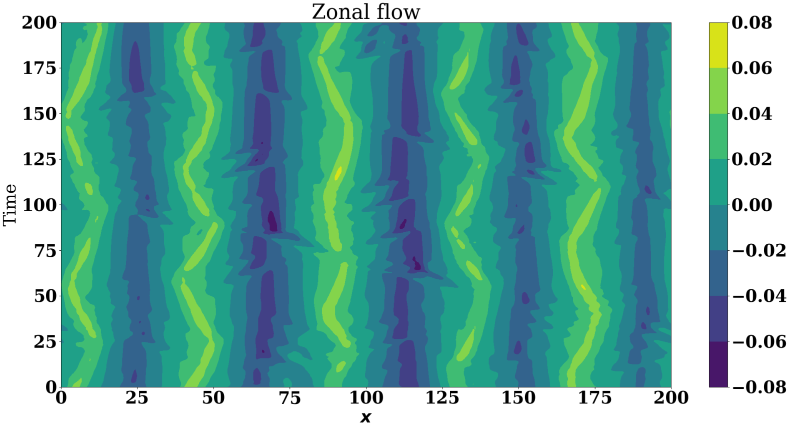

Figure: Zonal flows for $\chi = 1.2, \kappa_T = 2$.

Highly dissipative regime

Increasing collisionality leads to oscillating zonal fields

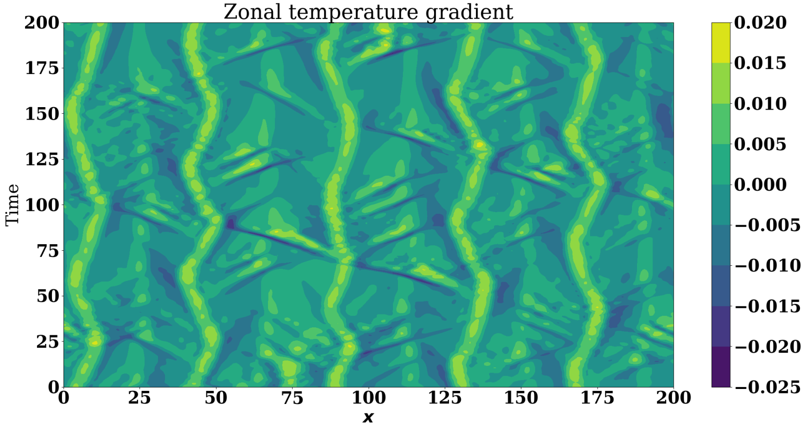

Figure: Zonal temperature for $\chi = 1.2, \kappa_T = 2$.